

Research article

Simultaneous access to different types of volume changes and the degree of cure during isothermal polymerization of polymer networks

Andreas Klingler^{*ID}, Maurice Gilberg, Bernd Wetzel^{ID}, Jan-Kristian Krüger

Leibniz-Institut für Verbundwerkstoffe, TU Kaiserslautern, Erwin Schrödinger Straße 58, 67663 Kaiserslautern, Germany

Received 29 April 2022; accepted in revised form 12 July 2022

Abstract. The current paper addresses the network-formation process of an epoxy polymer focussing on transition phenomena like the percolation threshold and the chemically induced glass transition. Based on a single type of measurement, different kinds of volume changes are used as sensitive probes to the morphological changes accompanying the polymerization process. Thereby, the rather new experimental technique of ‘Temperature Modulated Optical Refractometry’ (TMOR) allows to simultaneously obtain not only the volume shrinkage and the accompanying dynamic thermal volume expansion in the course of polymerization, but also the chemical turnover as a function of the refractive index. In order to test the applicability of the refractive index as a reasonable quantity to substitute respective infrared spectroscopy (IR) measurements, the network-formation is induced by homopolymerization reactions to specifically limit the degree of cure to a single spectral IR component. This countercheck is performed using IR by attenuated total reflection (ATR). Whereas the chemical-induced glass transition is clearly evidenced by the different kinds of volume changes, the percolation transition does not couple to these properties. However, the transition to the glassy state is highly variable and leads to large differences of the macro-molecular-induced morphologies.

Keywords: thermosetting resins, temperature modulated optical refractometry, infrared spectroscopy, degree of cure, glass transition

1. Introduction

Today, cross-linking polymers (thermosets) are amongst the most important functional and structural design materials. They are used as adhesives [1] or coatings [2], or are applied as polymer matrices in high performance applications for air- and spacecraft [3, 4]. The synthesis of these materials starts usually at a low molecular liquid state and undergoes a complex, non-equilibrium type of polymerization process. Thereby, the polymerization reaction is accompanied by severe irreversible changes of physical and chemical properties, comprised of a continuous succession of metastable states. The simultaneously progressing changes of the different chemical and physical

properties, such as the volume, the elastic moduli, the specific heat capacity or the degree of cure, reflect the ongoing course of the underlying polymerization process, yet from different perspectives. This process is the irreversible formation of chemical bonds, whereas the number of bonds can be interpreted as the natural order parameter. The sequence of these metastable states in the case of polymerization is of stochastic nature and manifests itself in permanent changes of the morphology and thus macroscopic variations of properties, such as *e.g.* the glass transition [5, 6].

Unfortunately, gaining access to these properties, and thus to the polymerization process, is challenging

^{*}Corresponding author, e-mail: andreas.klingler@ivw.uni-kl.de
© BME-PT

and most often limited to a measurement method that exclusively maps the desired property. With regard to chemical properties, the investigation of the chemical turnover (or degree of cure) by means of infrared spectroscopy (IR by attenuated total reflection) is well-known [7, 8]. However, the deduction of the degree of cure based on the analysis of IR spectra is often reduced to the evaluation of only one distinct absorption band, even though further absorption processes might be involved. Amongst physical properties, the specific heat (*e.g.* via temperature modulated calorimetry) [9, 10], the dielectric constants (*e.g.* via electrical impedance spectroscopy) [11] or (thermo-) mechanical properties (*e.g.* via rheology) [12] are most commonly used to characterize the polymerization process. Also, yet rather often neglected, the progress of polymerization can be assessed by monitoring accompanied types of volume changes (*e.g.* volume shrinkage or the thermal volume expansion) [13–15]. Unfortunately, all these latter types of susceptibilities view the polymerization-induced morphological changes as a function of time, and not as a function of the degree of cure. From an experimental perspective, the simultaneous acquisition of the aforementioned chemical and physical properties, like the degree of cure and the volume changes, in the whole course of polymerization would be of huge interest, especially with regard to continuous data acquisition from the liquid- to the viscoelastic- and solid state.

In recent papers of Müller *et al.* [8] and Philipp *et al.* [14] it was demonstrated that the refractive index, in the course of polymer network-formation can be a measure to both, volume changes (shrinkage) and the degree of cure. Thereby, the authors were able to reveal a partial proportionality between both parameters. Here, it should be stressed that the refractive index is related to the dielectric susceptibility ϵ measured at optical frequencies. However, the sole analyses of the refractive index or the degree of cure does not provide any insights into the dynamics of polymerization-induced freezing processes of a polymer system, and thus to *e.g.* the glass transition. Accessing such relaxation phenomena via volume changes in the course of polymerization is possible by probing a sample via a sinusoidal temperature perturbation. This allows measuring the dynamic thermal volume expansion, based on the underlying anharmonicity of the average molecular interaction potential [16, 17]. Generally, polymer genesis is best studied under

isothermal conditions, such that other extrinsic influences, as *e.g.* kinetic effects, are omitted. However, assessing the static thermal volume expansion under isothermal conditions is not possible, and along with that, relaxation phenomena stay usually hidden in the course of polymerization. The rather new technique of ‘Temperature Modulated Optical Refractometry’ (TMOR) is based on classical (Abbe) refractometry but additionally overcomes its limitations. The application of a low frequency and low amplitude temperature perturbation, enables TMOR to provide, in addition to the refractive index and the polymerization-induced volume shrinkage, access to the dynamic thermal volume expansion behaviour during polymer genesis, and thus to *e.g.* the polymerization-induced glass transition [13, 14, 18–21], even under isothermal conditions.

In this study, we combine such TMOR measurements with infrared spectroscopy (IR-ATR) to assess the degree of cure spectroscopically and to test the applicability of the refractive index as a quantity to substitute IR measurements. To be able to establish such a relationship between the refractive index and the degree of cure, thus relate polymerization-induced volume changes to the depletion of a specific molecular group, the network-formation is induced by homopolymerization of a diglycidyl ether of bisphenol A (DGEBA) resin. Thereby, the polymerization is initiated by small concentrations of 1-methylimidazole. This specifically limits the polymerization reaction to a single spectral IR component and allows us to relate the volume changes during homopolymerization solely to the DGEBA-dominated molecular network build-up process. In total, it is demonstrated that a multiplicity of important information to assess and describe polymerization-induced transition phenomena like the percolation threshold and the chemically induced glass transition can be described as a function of the degree of cure (*i.e.* the refractive index), all simultaneously gained from the same measurement.

2. Methodology

2.1. Reaction mechanism

The homopolymerization reaction of DGEBA is comprised of (i) an initiation reaction and (ii) a subsequent, rather complex, polymer network formation [22–25]. During the initiation stage, a highly nucleophilic adduct or zwitterion is formed that, subsequently, undergoes further cross-linking reactions (shown in Figure 1 for 1-methylimidazole and a

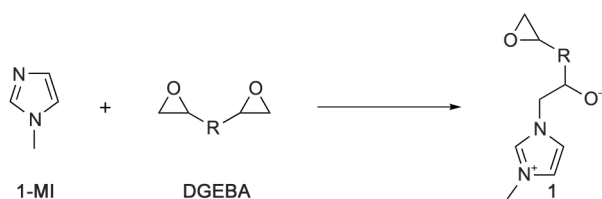


Figure 1. Initiation reaction of 1-methylimidazole (1-MI) and a DGEBA monomer, without hydroxyl catalysis, to form an adduct that can further initiate a cross-linking reaction (1).

diglycidyl ether of bisphenol A molecule (DGEBA), without hydroxyl catalysis).

This two-step process includes (i) intermolecular and intramolecular *N*-dealkylation reactions, leading either to linear chain growth or a cyclisation of molecules [24, 25], (ii) regeneration reactions of the initiator (β -elimination) [23], which allows to reuse the initiator molecule for further initiation reactions, (iii) or catalytic effects on initiation and polymerization, originating from hydroxyl groups [26, 27]. Figure 2 shows a possible polymerization route of the initially created adduct (1, cf. Figure 1) with a DGEBA molecule. Possible reactive pathways are e.g. a linear polymerization route (2 to 3) or the formation of crosslinks (3 to 4), depending on the oxirane ring structure that is attacked.

This multiplicity of reactive pathways is comprehensively summarized by Fernández-Francos [23] and demonstrates the underlying complexity of the network formation that are far too often taken as

granted, yet, which are the origin of the morphological varieties of interest.

2.2. Materials and sample preparation

In the present work a bifunctional diglycidyl ether of bisphenol A (DGEBA) based epoxy resin (Biresin CR144, Sika Deutschland GmbH, Stuttgart, Germany, average molecular weight $M_w = 374$ g/mol) is homopolymerized using different concentrations of 1-methylimidazole as an initiator (1-MI, DY070, Huntsman Corp., Salt-Lake City, USA, average molecular weight $M_w = 82.1$ g/mol). The mass concentrations were 0.9, 1.8 and 3.2 wt% (parts by weight of 1-MI to 100 parts by weight of the resin), which correspond to imidazole concentrations of about 2.0, 4.1 and 7.3 mol% (moles of imidazole per 100 moles of epoxide groups). Samples were mixed at room temperature with a dissolver aggregate for 20 min until an optically homogeneous mixture had been obtained. The samples are designated according to the 1-MI concentration used, i.e. DGEBA/MI-0.9, DGEBA/MI-1.8 and DGEBA/MI-3.2.

2.3. Infrared spectroscopy

Infrared spectroscopy was used as a tool to determine the chemical conversion of the different materials. Respective measurements were performed using the technique of attenuated total reflection (ATR) on a Nicolet iS50 (Thermo Fisher Scientific, Waltham, USA). The device was attached to a Rheonaut module

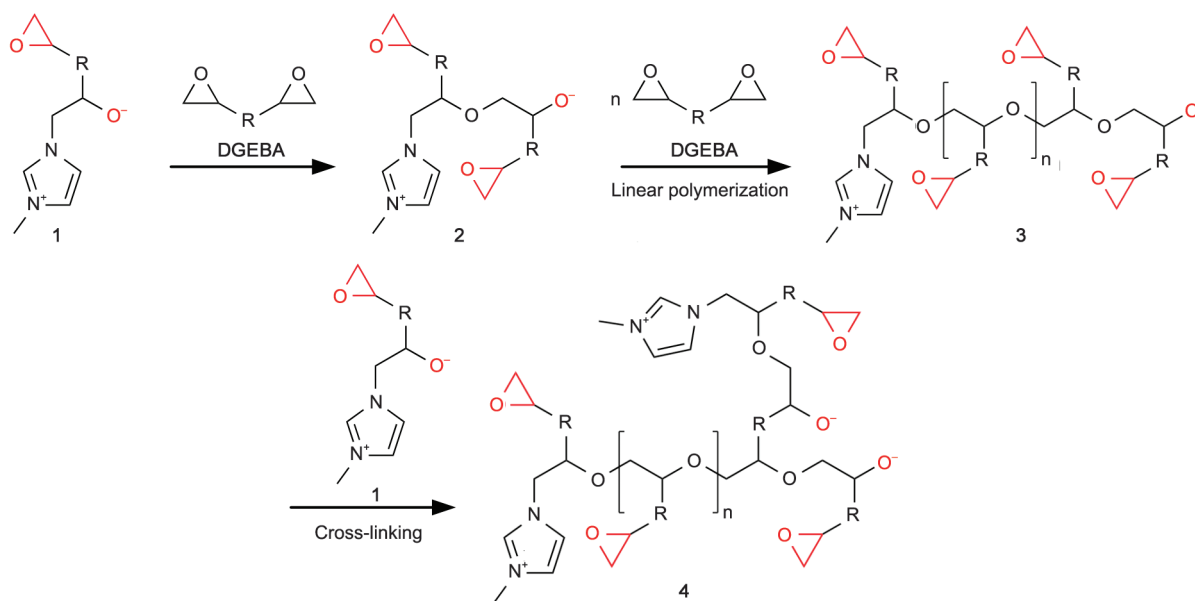


Figure 2. Possible homopolymerization route of DGEBA: (1) initiated by 1-methylimidazole-DGEBA adduct, (2) and (3) subsequent linear polymerization of DGEBA, (4) cross-linking of linear oligomers by reaction with (1), red: groups that potentially undergo polymerization.

(Haake Mars, Thermo Fisher Scientific, Waltham, USA), which provides a heating stage with an embedded diamond as a measuring prism. This setup allows measuring IR spectra in a temperature range from room temperature to 400 °C, either under isothermal conditions or under the influence of a superimposed heating rate. The measurements were conducted, isothermally, at $T_{\text{iso}} = 80\text{ °C}$. Once, the heating stage had reached the anticipated temperature, a sample of the liquid and reactive mixture was poured onto the measuring prism. Simultaneously, data acquisition was started. Every 30 seconds one (1) IR spectrum was recorded, which was the average out of eight (8) IR spectra, taken within four (4) seconds. The total measuring time varied in between 180 to 360 min, depending on the accelerator concentration. The number of spectra varied between 360 to 720, respectively.

For determining the chemical conversion of the different materials, the band heights, *i.e.* the intensities associated with the oxirane band $h_{\text{Ox}}(t)$ (at $\tilde{\nu} = 914\text{ cm}^{-1}$) and the aromatic backbone molecules $h_{\text{Ph}}(t)$ (phenylene band at $\tilde{\nu} = 1505\text{ cm}^{-1}$) were investigated [8, 28, 29]. The intensity of the oxirane band signal is a measure of the number of epoxied groups potentially available for initiation of the polymerization and subsequent homopolymerization (cf. Section 2.1.). Hence, the degree of cure u , and thus the reduction of the intensity of the oxirane ring band, is a time and polymerization driven process. On the other hand, the band height of the phenylene structure is considered as unaffected by the polymerization

process. Other effects, such as *e.g.* atmospheric influences on the measuring signal can affect the peak heights, and are accounted for by relating the height of the spectral line of the oxirane ring to the height of the spectral line of the phenylene ring.

For data analyses, the background signal was fitted using a spline-fit function. The peaks of the oxirane ring structure and the phenylene were fitted using a Gauss-fit function. The degree of cure u was determined based on Equation (1):

$$u(t) = 1 - \frac{\frac{h_{\text{Ox}}(t)}{h_{\text{Ph}}(t)}}{\frac{h_{\text{Ox}}(t_0)}{h_{\text{Ph}}(t_0)}} \quad (1)$$

The initial peak intensities at t_0 were determined at $t = t_0 = 2\text{ min}$, to allow temperature equilibration of the sample.

2.4. Abbe refractometry and TMOR

The underlying measuring principle of TMOR [18, 30] is Abbe refractometry, which measures the angle α_{tot} of total internal reflection at the interface between a prism of known refractive index n_{prism} and the optically homogeneous and transparent sample. The prism is made of neodymium-doped yttrium aluminum garnet (YAG) or sapphire.

Applying Snellius law the refractive index n_{sample} of the sample can be calculated for the given optical wavelength λ and the temperature T at ambient pressure.

Modern Abbe refractometry (Abbemat 550, Anton Paar OptoTec GmbH, Seelze, Germany),

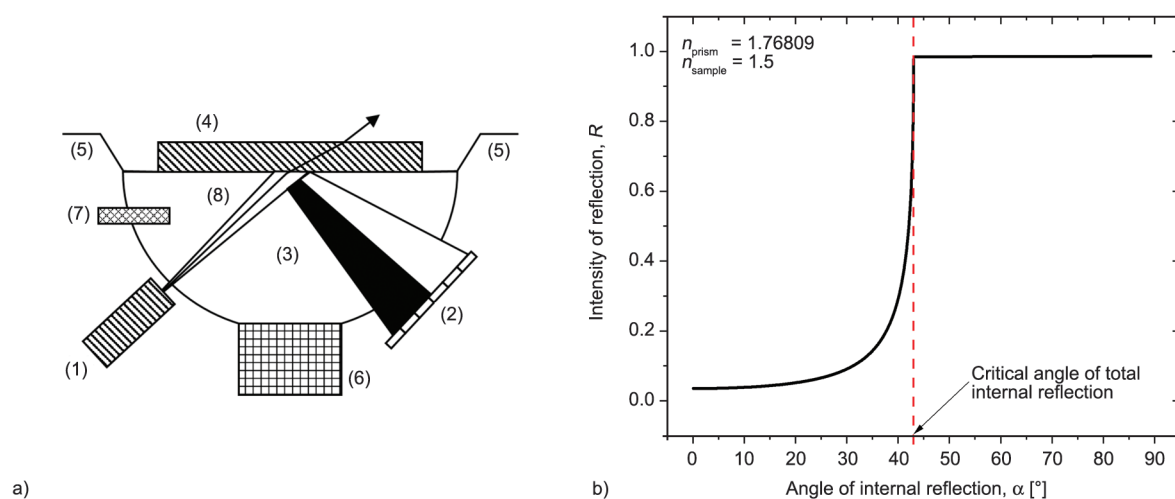


Figure 3. Principles of the Abbe refractometry and TMOR measurement technique: a) (1) light source for $\lambda = 589\text{ nm}$ (Na-D spectral line), (2) diode array sensor, (3) measurement prism, (4) sample with $n_{\text{sample}} = n_2$, (5) sample cavity, (6) temperature controller, (7) temperature sensor, (8) divergent yet monochromatic light beam. b) s-polarized Fresnel curve. R reflection coefficient, α angle of incidence.

schematically given in Figure 3a, measures the s-polarized Fresnel curve (Figure 3b). This Fresnel curve is detected with a diode array (Figure 3a (2)) and the refractive index $n = n_{\text{sample}}$ is derived from the fit of this curve. Based on measurements of n , the quantity N_{mean} is defined as the sliding average over one modulation period by the Abbemat 550 instrument (without influence of the operator). It is the quantity N_{mean} , which is discussed when the refractive index is addressed in the current paper. The relative and absolute accuracy of $\Delta N_{\text{mean}}/N_{\text{mean}}$ are 10^{-6} and 10^{-5} respectively.

The temperature control (6) in Figure 3a, allows for a temperature accuracy of $\Delta T = \pm 0.03$ K of the prism and the adjacent probed sample volume.

After sample preparation, the liquid and reactive mixtures were poured onto the pre-heated measuring prism of the refractometer. All measurements are performed under isothermal conditions at $T_{\text{iso}} = 80$ °C and constant pressure, *i.e.* N_{mean} only depends on the internal variable $(u(t))_{T_{\text{iso}}}$. In the present work, the temperature amplitude ΔT is 0.1 K, the temperature-induced relaxation dynamics are probed at a low frequency of $f = 17$ mHz, corresponding to a modulation period of $\tau = 60$ s. The measured N_{mean} data are automatically recorded in a computer file as a table (t, N_{mean}) where t corresponds to the time of measurement.

Note, for measuring reasons data acquisition starts only after two minutes, after the start of the measurement. Hence, all events, such as temperature induced heating rate effects due to temperature equilibration of the ~ 0.15 ml sample on the hot prism surface, are not captured within the datasets.

3. Results and discussion

The homopolymerization of a DGEBA resin is a complex combination of linear chain growth and cross-linking reactions, regeneration reactions of the initiator species or even termination reactions of single polymerization processes, cf. Section 2.1 or [23]. Thereby, the underlying processes largely depend on the initial initiator concentration. In the case of very low initiator concentrations, the formed adducts (cf. Figure 1) are far apart from each other, *i.e.* the chances of immediate interactions between these reactive adducts are extremely limited in order to form cross-links (cf. Figure 2). Considering such rather theoretical conditions, subsequent polymerization reactions are likely to start via linear chain growth.

Assuming one single initiator specie could be introduced into the DGEBA system, and regeneration reactions would be omitted, such a homopolymerization reaction could yield to the formation of an extremely large single polymer chain. On the contrary, when high initial initiator concentrations prevail in the DGEBA resin, interactions between initiated moieties increase and along with that the number of cross-linking reactions. At the other extreme, when the 1-MI concentration reaches such a degree that the number of formed adducts is equal or exceeds the number of remaining DGEBA molecules, cross-linking might even be stopped, and low molecular, liquid, non-cross-linkable oligomers remain, since reactive partners are missing [31]. Even more, if one additionally considers that these processes are not unique to a certain DGEBA/1-MI composition and sample, but can also occur simultaneously in the same sample, *e.g.* driven by local differences of the 1-MI concentration and eventually provoked by externally induced heat flux, it becomes obvious, how complex and difficult it is to predict and derive macromolecular properties of such polymer systems. However, common to all these mechanisms, in the course of polymerization, is that they are represented by volume changes. Hence, investigating this physical property, not only as a measure to shrinkage, but also via the refractive index as a natural order parameter to the degree of cross-linking seems a reasonable pathway in order to peak behind the complex molecular processes during homopolymerization.

3.1. TMOR and IR – access to the degree of cure and the dynamic glass transition

For practical reasons, measurements of physical or chemical properties in the course of polymerization are usually performed as a function of time, which is a poor measure to the progress of polymerization. A more valuable source of information about the progress of polymerization is the degree of cure, *i.e.* the level of the chemical turnover. Therefore, the abscissa of time has to be transformed to the degree of cure axis. To do this, a common experimental technique is infrared spectroscopy (IR, IR-ATR) [28, 29, 31]. Figure 4 shows a typical IR-ATR diagram for the spectroscopic conversion, u , of one of our model systems, DGEBA/MI-3.2 (dataset 3, indicated as subscript), at $T_{\text{iso}} = 80$ °C as a function of curing time (red, spherical data points). The degree of cure, u , starts by strongly increasing at the beginning of the

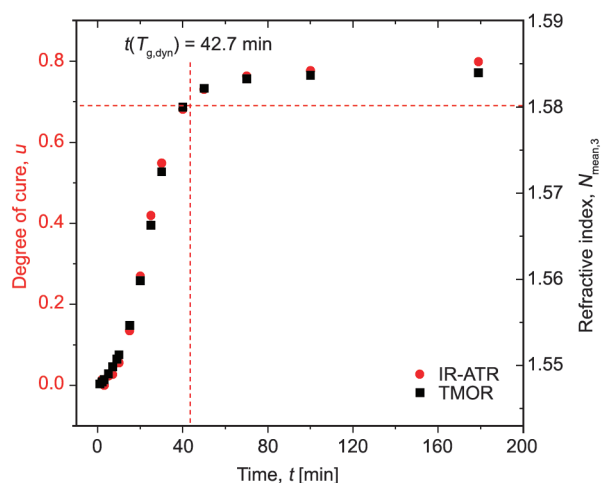


Figure 4. Homopolymerization of DGEBA/MI-3.2 at $T_{\text{iso}} = 80^\circ\text{C}$. Spectroscopic conversion u (red data points) and average refractive index N_{mean} (black data points) of one dataset (dataset no. 3, indicated as subscript) as a function of curing time. $t(T_{\text{g,dyn}})$ is the time when the chemically-induced, dynamic glass transition (based on β''_{max} , cf. Figure 7) is reached.

polymerization process and then bottoms out, reaching an incomplete or hindered state of polymerization at $u \sim 0.8$. However, the course of $u(t)$ does not provide any information about the type of polymerization. The measured degree of cure, based on the loss of oxirane rings, changes in the course of polymerization independent of a linear type of polymerization or a cross-linking process. In both cases, the number of oxirane rings diminishes.

Therefore, besides the chemical conversion over time, as seen by IR-ATR, Figure 4 shows additionally the evolution of the refractive index N_{mean} (measured independently by TMOR) as a function of time t , in the course of the polymerization of the sample DGEBA/MI-3.2 (black, squared data points). The similarity of both measurements is striking. This apparent resemblance between $u(t)$ and $N_{\text{mean}}(t)$ suggests the existence of a similarity-transformation between both quantities, which is not only limited to the current epoxy/initiator system, as discussed below. Thus, the question appears in which way the refractive index N_{mean} is related to the formation of chemical bonds or the annihilation of reactive groups. To elucidate this relationship, it is necessary to analyse the Lorentz-Lorentz relationship [32–34] (Equation (2)):

$$N_{\text{mean}} = \sqrt{\frac{1 + 2 \cdot r \cdot \rho}{1 - r \cdot \rho}} \quad (2)$$

where r corresponds to the specific refractivity and ρ to the mass density of the sample. The mass density ρ is proportional to the electronic dipole density of the material under consideration and r reflects the average magnitude of the electronic dipole moments. Hence, polymerization-induced changes of N_{mean} are caused by a polymerization-induced molecular densification of the electronic dipole system, *i.e.* the material shrinks, and the annihilation and creation of electronic dipoles due to the formation of new chemical bonds is accompanied by the loss of oxirane rings. In other words, the chemical reaction, *i.e.* the change of chemical bonds, which is measured by the loss of the oxirane rings, leads to a densification of the polymerizing material and to the loss and creation of new dipoles.

If N_{mean} can be defined as a function of the chemical turnover u , based on the Lorentz-Lorentz equation, two independent coefficients $\beta(u)$ and $\psi(u)$ can be related to the first derivative of $N_{\text{mean}}(u)$ [18] (Equation (3)):

$$\frac{-6N_{\text{mean}}(u)}{(N_{\text{mean}}^2(u) - 1)(N_{\text{mean}}^2(u) + 2)} \cdot \frac{dN_{\text{mean}}}{du} = \psi(u) + \beta(u) \quad (3)$$

with (Equation (4) and (5)):

$$\beta(u) = \beta_{\text{sh}}(u) = -\frac{1}{\rho} \frac{d\rho}{du} \quad (4)$$

$$\psi(u) = -\frac{1}{r} \frac{dr}{du} \quad (5)$$

where $\beta = \beta_{\text{sh}}$ is called the ‘shrink coefficient’ and ψ defines the relative change of the specific refractivity due to changes of chemical bonds. If the changes of ψ are small in comparison to those of β , *i.e.* $\psi \ll \beta$, the changes dN_{mean}/du are predominantly caused by the polymerization-induced volume shrinkage.

Taking the similarity between $u(t)$ and $N_{\text{mean}}(t)$ into account, it is self-evident to eliminate the time coordinate t in both datasets in order to create a direct relationship between both quantities, as shown in Figure 5.

The polymerization process, as reflected by the degree of cure u , ends at about $u_{\text{EP}} \sim 0.8$ (further discussion see below), whereas the full turnover ($u = 1$) is based on a three hour-post curing process at 140°C . After the post-curing process, the relevant spectral peak intensity was evaluated and set to 100%. As expected from Figure 4, the presentation

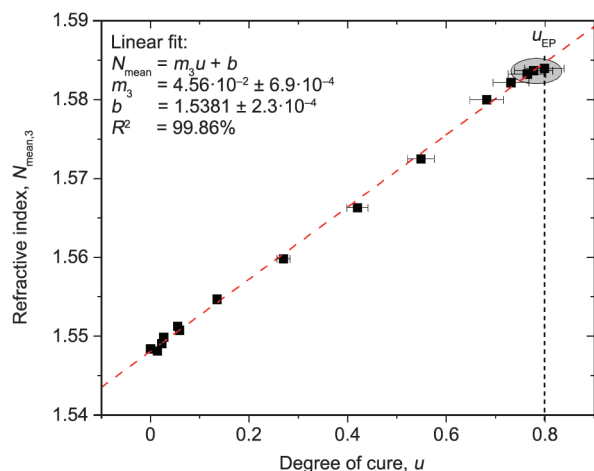


Figure 5. Relationship between the refractive index N_{mean} and the spectroscopically measured degree of polymerization u of DGEBA/MI-3.2 (dataset 3, indicated as index). u_{EP} indicates the end of polymerization for the applied isothermal condition $T_{\text{iso}} = 80^\circ\text{C}$. A total error of 5% of the degree of cure is indicated [8].

of N_{mean} versus u in Figure 5 behaves widely linear. However, for $u > 0.75$, N_{mean} seems to slightly level off. This feature, at such a large chemical turnover in the course of the $N_{\text{mean}} = N_{\text{mean}}(u)$ -plot, might be either indicative for the chemically induced glass transition or simply be related to data scatter. As a matter of fact, at least at the end of the polymerization process all samples were found to be in a solid state, indicating the existence of a quasi-static glass transition ($T_{\text{g}}^{\text{stat}}$). In the case the dataset at the end of the measurement is indeed bending (and would not be an artefact due to data scatter), this behaviour would indicate that the polymerization-induced glass transition most-likely hinders further volume changes while the polymerization continues. Such a bending behaviour of N_{mean} , or the volume shrinkage, over the degree of cure was already reported by Müller *et al.* [8] and others [14, 15, 35]. From the perspective of volume changes (cf. Equation (2)), Wenzel [35] stated that an off-levelling of the volume shrinkage as a function of the degree of cure, in his case for an epoxy/anhydride system, might indeed be related to the glass transition of the system. Wenzel did not observe this behaviour for resin/ hardener systems that did not reach a glassy state, due to non-stoichiometric mixtures. On the other hand, Holst *et al.* [15], who performed similar investigations, did not find ‘significant deviations’ from linearity in the course of volume changes over the degree of cure, even though, one could speculate on such a bending behaviour

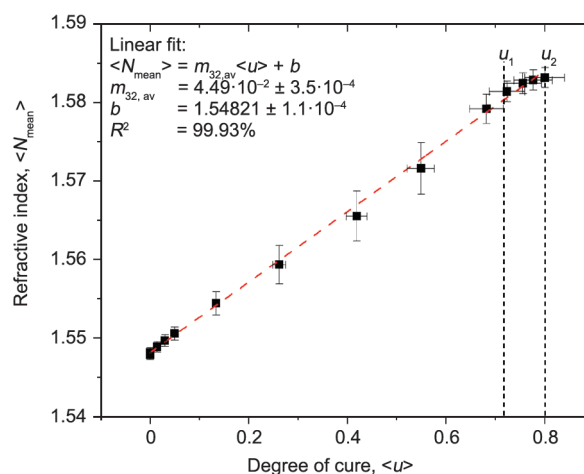


Figure 6. Relationship between the average refractive index $\langle N_{\text{mean}} \rangle$ and the average spectroscopically measured degree of polymerization $\langle u \rangle$ of DGEBA/MI-3.2. u_1 corresponds to the degree of cure at the loss maximum of β''_{max} ($f = 17$ mHz) given in Figure 7. u_2 corresponds to the maximum reachable chemical turn-over, under the given conditions. A total error of 5% of the degree of cure for u is indicated.

based on their data. However, in the present case, the data accuracy of Figure 5 is insufficient to confirm the glass transition-induced bending hypothesis.

To test the statistical relevance of the linear relationship between N_{mean} and u , on one hand, and the seemingly bending behaviour of the $N_{\text{mean}}(u)$ function close to the end of the polymerization process, on the other, the $N_{\text{mean}}(t)$ dataset was independently measured six times and the degree of cure (via IR) four times. The results are shown in Figure 6.

In the margin of error the averaged $\langle N_{\text{mean}} \rangle$ as a function of the averaged turnover $\langle u \rangle$ is still linear in the complete $\langle u \rangle$ -interval. However, interestingly, the polymerization process, reflected by the average chemical turn-over $\langle u \rangle$, ends at around $u_2 = u_{\text{EP}} \sim 0.8$. Hence, something must hinder the further evolution of the polymerization process at the isothermal polymerization temperature of $T = 80^\circ\text{C}$. This could indeed be the above mentioned polymerization-induced glass transition, which would strongly restrict the translational, rotational and conformational molecular mobility of the constituents. However, neither the refractometry measurements nor the IR measurements, presented and discussed so far, prove the existence of a glass transition.

As indicated as u_1 in Figure 6, for DGEBA/MI-3.2, dataset 3, the polymerization-induced dynamic glass transition ($f = 17$ mHz, s.a. below) takes place at

$u_1 = 0.71$. Around u_1 , which still reflects a viscoelastic state of DGEBA/MI-3.2, it remains unclear whether the polymerization-induced shrinkage can be hindered although the polymerization proceeds. Since the probe frequency of $f = 17$ mHz is rather low, one can indeed imagine such a behaviour. This would mean, in the apparently bended region of N_{mean} a superordinate network structure would have been frozen, already. However, very localized, further polymerization reactions could still occur, even though they slowly diminish and stop at $u_2 \sim 0.8$.

As mentioned before, Abbe refractometry under isothermal polymerization conditions is not able to yield information about polymerization-induced freezing phenomena. A physical quantity, which would prove the presence of the polymerization-induced glass transition is the dynamical thermal volume expansion coefficient β^* ($= \beta' - i\beta''$). This quantity can be accessed via the recently developed ‘Temperature Modulated Optical Refractometry’ (TMOR). TMOR [18, 30] is based on Abbe refractometry (cf. Section 2.4.) and extended by a temperature controller (cf. Figure 3a, (6)) which is able to modulate the sample temperature close to the prism by superimposing a sinusoidal temperature signal, T^{mod} , on the average temperature of the sample T_{iso} (Equation (6)):

$$T(t) = T_{\text{iso}} + T^{\text{mod}} = T_{\text{iso}} + A^T \sin(2\pi ft) \quad (6)$$

where $T(t)$ is the instantaneous temperature, A^T and f are the amplitude and the frequency of the sinusoidal modulation of temperature, respectively. In order to disturb the polymerization kinetics as little as possible, the amplitude of the temperature modulation is selected as low as $A^T = 0.1$ K. The theoretical background of the TMOR technique has been described in detail in literature (e.g. [14, 18–20, 30]) and therefore it will be introduced only shortly in the current paper.

The refractive index response due to the temperature excitation (Equation (6)) can be well described by the following model in the framework of linearized irreversible thermodynamics [16] (Equation (7)):

$$(n(t))_u = (N_{\text{mean}})_u + (A^n)_u \sin(2\pi ft - (\Phi)_u) \quad (7)$$

where N_{mean} denotes the mean refractive index response of the sample, calculated using a moving average over one modulation period (see also Section 2.4.), A^n is the amplitude of the sinusoidal

refractive index response to the temperature perturbation, and Φ is the phase lag between the sinusoidal temperature perturbation and the refractive index response.

The dynamic thermal expansion coefficient $\beta^*(t)$ is determined simultaneously and yields details about phase transitions from the liquid state, over the percolation to the glassy state, even under isothermal conditions. The dynamic thermal volume expansion coefficient $\beta^*(t, T_{\text{iso}}, f) = \beta'(t, T_{\text{iso}}, f) + i\beta''(t, T_{\text{iso}}, f)$ can be quantified according to (Equations (8) and (9)):

$$(\beta')_u = \frac{-6(N_{\text{mean}})_u}{\left[(N_{\text{mean}})_u^2 - 1\right]\left[(N_{\text{mean}})_u^2 + 2\right]} \cdot \frac{(A^n)_u}{A^T} \cos((\Phi)_u) \quad (8)$$

$$(\beta'')_u = \frac{-6(N_{\text{mean}})_u}{\left[(N_{\text{mean}})_u^2 - 1\right]\left[(N_{\text{mean}})_u^2 + 2\right]} \cdot \frac{(A^n)_u}{A^T} \sin((\Phi)_u) \quad (9)$$

For the sake of simplicity, we omit the index u in the following. In the absence of dynamics, or for very low modulation frequencies, β' yields the static thermal volume expansion coefficient β_{stat} . In the present work, the temperature-induced relaxation dynamics are probed at a low frequency of $f = 17$ mHz, corresponding to a modulation time of $\tau_{\text{mod}} = 60$ s. The time scale of the dynamic probe may come in conflict with polymerization when the polymerization progress is too fast. A proper evolution of a neat sinusoidal signal $n(t)$ is therefore a precondition for the determination of $\beta^*(t)$. This limits the possibility to determine $\beta^*(f, t)$ with TMOR at large rates of polymerization.

Figure 7 shows the real and imaginary part of the dynamic thermal volume expansion coefficient, of DGEBA/MI-3.2 over time at $T_{\text{iso}} = 80^\circ\text{C}$.

The imaginary part β'' shows a clear maximum after $t(T_{\text{g,dyn}}) \sim 43$ minutes. At the same time the real part, β' , shows an inflection point and strongly decreases from about $6 \cdot 10^{-4}/\text{K}$ to about $1.5 \cdot 10^{-4}/\text{K}$. This change of the dynamic thermal volume expansion coefficients β' and β'' is typical for a polymerization-induced glass transition [18]. According to Figure 4 the temporal position of this glass transition $t(T_{\text{g,dyn}})$ is just below the levelling of N_{mean} , and according to Figure 5 and Figure 6 (cf. marked region), close to

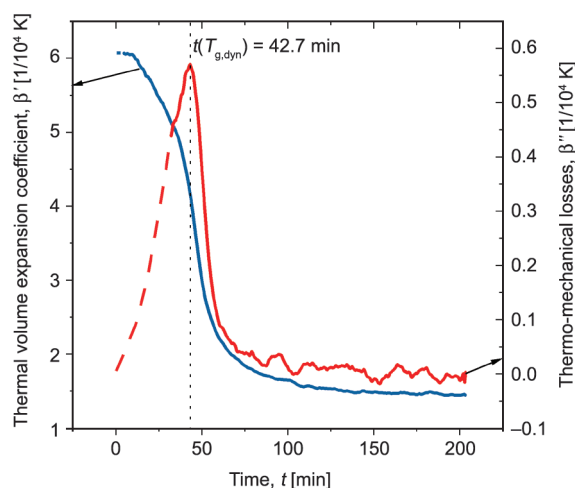


Figure 7. Real and imaginary part of the dynamical thermal volume expansion coefficient $\beta^* = \beta' - i\beta''$ of DGEBA/MI-3.2 (dataset 3), measured at $T_{\text{iso}} = 80^\circ\text{C}$ as a function of time. Dataset approximation (dashed lines) at the beginning of the measurement, due to the interference between velocity of the chemical conversion and dynamic probe frequency ($\tau_{\text{mod}} = 1/f = 60$ s). $T_{\text{g,dyn}} = 80^\circ\text{C}$ is reached after ~ 43 minutes and defines the dynamic glass transition temperature measured at a frequency of $f = 17$ mHz.

the end of the recorded $N_{\text{mean}} = N_{\text{mean}}(u)$ curve. The behaviour of N_{mean} in all datasets indicates that the end of the polymerization process is driven by a polymerization-induced glass transition. However, it should be kept in mind that the described glass transition phenomenon is of dynamical nature, *i.e.* the static solidification, which would strongly hinder further polymerization, occurs somewhat later after the peak of β'' in Figure 7.

3.2. Influence of 1-MI concentration on the polymerization process

As has recently been shown in [13], the amount of initiator species (1-MI) largely affects the network formation, under the perspective of volume changes of DGEBA. This leads to several questions regarding the influence of 1-MI on the polymerization process: i) does the 1-MI concentration affect the final degree of cure, as measured by the spectroscopic turnover u (loss of oxirane rings)? ii) to which extent does the degree of cure modify the refractive index N_{mean} , considering that the amount of 1-MI molecules might change the ratio between linear bond formation and cross-linking? And in turn, how does the type of bond formation affect the relationship between N_{mean} and the spectroscopic degree of cure u ?

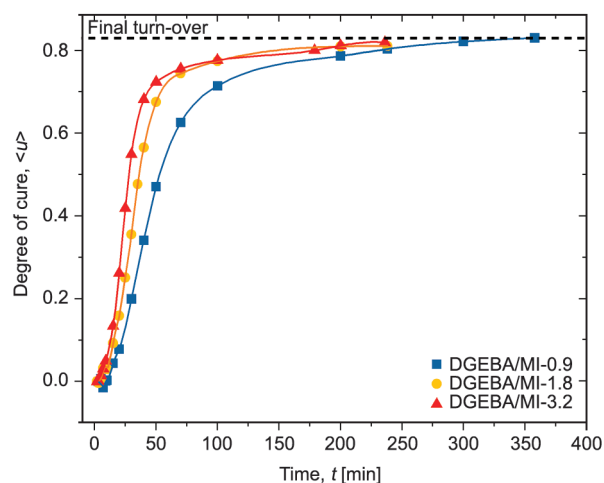


Figure 8. Average spectroscopic turnover $\langle u \rangle$ as a function of curing time measured at $T_{\text{iso}} = 80^\circ\text{C}$ for different mixtures of DGEBA with 1-MI.

iii) The polymerization-induced glass transition depends on the molecular arrangement during the network formation. How does this phenomenon become visible in the N_{mean} versus u -representation, if the 1-MI concentration changes?

To elucidate question (i) Figure 8 shows the average degree of cure $\langle u \rangle$ over time for three different DGEBA/MI systems. Obviously, and in the margin of error, the final spectroscopically measured degree of cure is independent of the 1-MI concentration. It levels off at around $u = 0.83$. In other words, independent of the type of polymerization (*i.e.* cross-linking vs. linear chain extension), the final degree of cure is neither enhanced nor restricted by the polymerization process, at least in the investigated 1-MI concentration range. Hence, the loss of oxirane rings is very similar for all material systems. In contrast, the time-related behaviour of the $\langle u \rangle(t)$ -curves strongly depends on the 1-MI concentration (see also (iii)).

With regard to question (ii) and as shown in Figure 9, in the margin of error, the electronic polarizability ($\langle N_{\text{mean}} \rangle$) seems not to be modified by the number of created and/or annihilated chemical bonds ($\langle u \rangle$). Based on the given datasets, nothing can be said about the ratio between the formation of cross-links and linear bonds. At the beginning of the polymerization process, $\langle N_{\text{mean}} \rangle$ ($\langle u \rangle$) follows a descending order with increasing 1-MI concentration. This behaviour is to be expected due to the molecular mixture of DGEBA ($n_{\text{T} = 80^\circ\text{C}} = 1.5477$) and 1-MI ($n_{\text{T} = 80^\circ\text{C}} = 1.4691$). Between $0.2 \leq \langle u \rangle \leq 0.7$ the data points for the different MI-concentrations

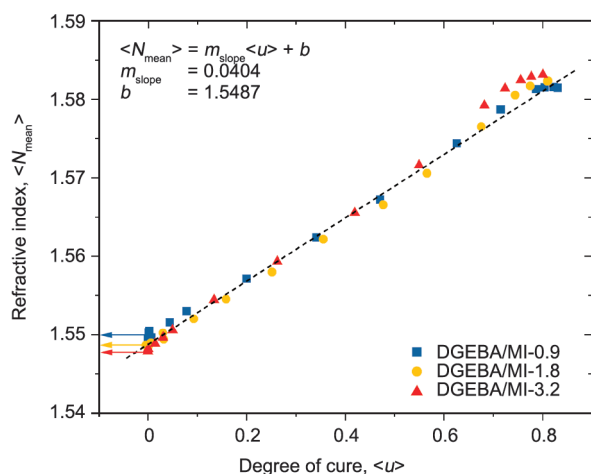


Figure 9. Relationship between the average refractive index $\langle N_{\text{mean}} \rangle$ and the spectroscopically measured degree of cure $\langle u \rangle$ of DGEBA, under the influence of three different concentrations of 1-MI: 0.9, 1.8 and 3.2, the dashed, linear slope serves as a guide to the eye.

merge, probably indicating the consumption of free 1-MI-molecules, as shown and discussed in [13]. Above $u > 0.7$, $\langle N_{\text{mean}} \rangle$ seems to level for all DGEBA/MI-systems. Thereby, in the margin of error, the levelling behaviour is rather undefined and independent of the 1-MI-concentration. Hence, the 1-MI-concentrations used for the current experiments neither influence the final degree of cure at the polymerization temperature of 80 °C (cf. also Figure 8), nor do they affect the levelling behaviour of the $\langle N_{\text{mean}} \rangle$ -data (Figure 9). Moreover, the linear transformation between $\langle N_{\text{mean}} \rangle$ and $\langle u \rangle$, within the scope of accuracy, is independent of the 1-MI-concentration.

It should be noted that the shown datasets are an average of several measurements, which all underlie certain measuring variabilities and uncertainties, such as e.g. the seemingly identical time scales of the independent measurements of the refractive index and the spectroscopically measured degree of cure. The latter one even underlies the challenge to properly interpret the base line for data evaluation. Coming to question (iii): According to the Lorentz-Lorenz relationship (Equation (2)), the levelling of $\langle N_{\text{mean}} \rangle$ at $u \geq 0.7$, has to be related to some kind of volume changes. Rearranging Equation (2), the volume shrinkage can be derived from N_{mean} (Equations (10) and (11)), in the whole course of polymerization, up to the final, levelled state, under the given isothermal conditions [13, 36]:

$$v_{\text{sh}} = \frac{v_{\text{ns}} - v_{\text{ns}, u=0}}{v_{\text{ns}, u_{\text{max}}}} \quad (10)$$

where:

$$v_{\text{ns}} = \frac{1}{r \cdot \rho} = \frac{N_{\text{mean}}^2 + 2}{N_{\text{mean}}^2 - 1}, r = 1 \quad (11)$$

Figure 10 displays a data plot of the derived volume shrinkage v_{sh} of the different DGEBA/MI systems as a function of the spectroscopically measured degree of cure $\langle u \rangle$. The maximum shrinkage between $u = 0$ and $u \sim 0.83$ changes gradually from 4.8 to 5.3% with increasing 1-MI-concentration. From the data scatter point of view, the hierarchy of the maximum shrinkage with respect to the 1-MI-concentration seems to be statistically relevant.

At the beginning of the polymerization process, the volume shrinkage overlaps for all three systems. Then, in the course of polymerization, the datasets start to deviate from each other and split up onto three different plateaus once the volume changes start to level, following the already mentioned descending order of maximum shrinkage with increasing 1-MI concentration. Hence, the volume shrinkage opposed to the levelling behaviour of $\langle N_{\text{mean}} \rangle$ over $\langle u \rangle$ (Figure 9) is a more sensitive measure to the effect of different 1-MI concentrations.

Volume shrinkage means an improved molecular packing and indicates a loss of translational and rotational degrees of freedom of molecules. The formation

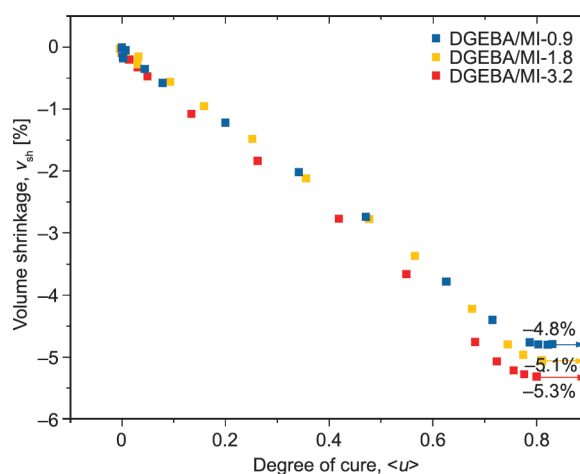


Figure 10. Volume shrinkage as a function of the spectroscopically measured degree of cure $\langle u \rangle$ of DGEBA, under the influence of three different concentrations of 1-MI: 0.9, 1.8 and 3.2. The dataset was derived from the N_{mean} data given in Figure 9.

of strong intermolecular bonds, in particular in the case of a three dimensional molecular network formation, is especially efficient in producing such losses. Following this argumentation, the maximum shrinkage hierarchy discussed above could indicate an increased cross-link density for materials with increased 1-MI-concentration. However, other types of strong molecular bonds between molecules and chains might influence or substitute the effect of cross-linking.

Comparing the datasets of Figure 9 and Figure 10, even the volume shrinkage could be considered as a measure to the degree of cure, if the linearity between degree of cure and volume shrinkage is taken into account.

So far, based on the analyses of $N_{\text{mean}}(t)$, $u(t)$ and $v_{\text{sh}}(t)$, it remains unclear if the levelling in the datasets correlates to the polymerization-induced glass transition. Therefore TMOR measurements were performed to supplement the already gained results by the dynamic thermal volume expansion coefficient $\beta^*(t)$, which is a sensitive property to freezing processes.

The dynamic thermal volume expansion coefficients, β' and β'' , as shown in Figure 7, are measured as a function of time and not as function of the chemical turnover u . In order to replace the time by the chemical turnover we can now simply replace the spectroscopically measured turnover u with the short time averaged refractive index N_{mean} , based on the above discussed similarity transformation. In Figure 11, the dynamic thermal volume expansion coefficient $\beta^*(f) = \beta'(f) - i\beta''(f)$ is shown as a function of the average chemical turnover $\langle u \rangle$ (top axis), as well as $\langle N_{\text{mean}} \rangle$ (bottom axis). The results obtained for the probe frequency $f = \omega/(2\pi) = 17$ mHz are striking: The real and imaginary parts, β' and β'' , behave as a function of the degree of cure, u , like a turnover-controlled glass relaxator. An amorphous polymer undergoing a thermal glass transition under cooling conditions would show a similar trend for β' and β'' [19, 37]. In both cases the glass transition is a result of the randomly closed packing of the molecular system [5, 38], and the drop of the dynamic thermal volume expansion coefficient β' is a canonical precursor for the glass transition. The interpretation of a polymerization-induced glass relaxator [5] is in line with the correlation between the linear part of $\beta'(u)$ and a quasi-static thermal volume expansion coefficient $\beta(u)$ with $\omega\tau \ll 1$, where τ is the main relaxation

time of the glass-forming process and $f = \omega/(2\pi)$ is the thermal probe frequency. In contrast to literature [39], as a consequence of the strict linearity of the $\beta'(u) \sim \beta(u)$ -dataset, until the onset of the dynamic glass transition and in the margin of error, any evidence for a percolation phase transition can be ruled out. From the perspective of the shear stiffness, the percolation threshold becomes visible as a second order phase transition and is extremely important when designing applications based on cross-linked polymers. Taking the shear stiffness $G(u)$ as an order parameter susceptibility, there seems to be no coupling between $G(u)$ and $\beta(u)$. The slightly decreasing linear part, in the region of $\omega\tau < 1$ of $\beta' = \beta'(u)$ suggests that the anharmonicity of the average intermolecular interaction potential at the polymerization temperature of $T_{\text{iso}} = 80$ °C decreases continuously from the liquid to the viscoelastic state, with an increasing degree of cure. In the course of polymerization, when the polymer system undergoes a transition to the glass state, the thermal volume expansion is dominantly caused by anharmonic vibrations [16].

Another result obtained from Figure 11 is the fact that within the linear range of $\beta'(u)$ the quasi-static thermal volume expansion is almost independent of the 1-MI concentration. Taking into account that the ratio between cross-links and linear molecular bonds might increase with the 1-MI concentration, it appears that, in the margin of error, $\beta'(u)$ does not depend on this ratio. This is also true for each system on its own. Hence, in the course of polymerization, up to $u < 0.7$, the thermal volume expansion β' seems to be independent of the type of polymerization (linear bond formation vs. cross-linking).

The rather large thermomechanical losses, reflected by $\beta''(u)$ in the linear range of $\beta'(u)$ have nothing to do with the glass relaxation (α -process), instead they are rather caused by hydrodynamic friction between the polymer material and the optical prism surface in the refractometer [19].

The three horizontal bars in Figure 11 indicate the N_{mean} -interval (*i.e.* the degree of cure), in which the dynamic glass transition, based on β''_{max} of up to six individual measurements of DGEBA/MI-0.9, -1.8 and -3.2 varied. In the range of the applied 1-MI concentrations, the dynamic glass transitions largely overlap. For a more detailed view on the variation of individual measurements of the same material batch see the data collection of DGEBA/MI-1.8 in Figure 12.

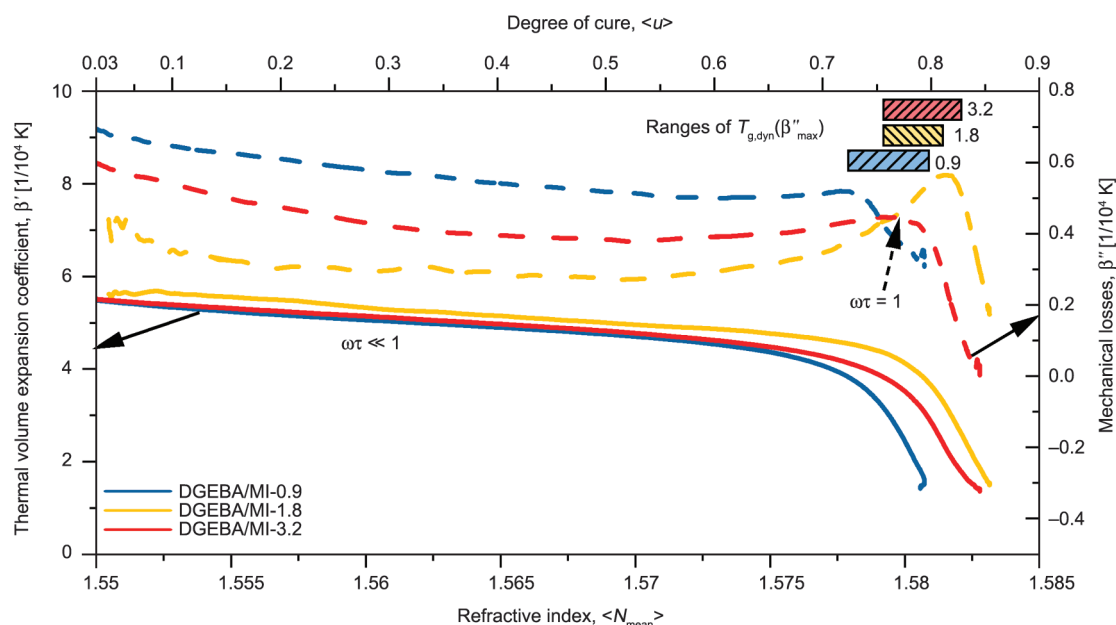


Figure 11. Dynamic thermal volume expansion coefficient β' and thermo-mechanical losses β'' as a function of $\langle N_{\text{mean}} \rangle \sim \langle u \rangle$, of exemplary datasets of DGEBA/MI-0.9, -1.8 and -3.2, $f = 17$ mHz ($\omega = 2\pi f$), $T_{\text{iso}} = 80^\circ\text{C}$. The horizontal bars show the N_{mean} -interval in which the dynamic glass transitions of up to six individual measurements of DGEBA/MI-0.9, -1.8 and -3.2 vary. The degree of cure $\langle u \rangle$ is based on the linear relationship of $\langle N_{\text{mean}} \rangle$ and $\langle u \rangle$ given in Figure 9. The dynamic glass transition temperature $T_{g,\text{dyn}}$ corresponds to $T_{\text{iso}} = 80^\circ\text{C}$ at $\omega\tau = 1$.

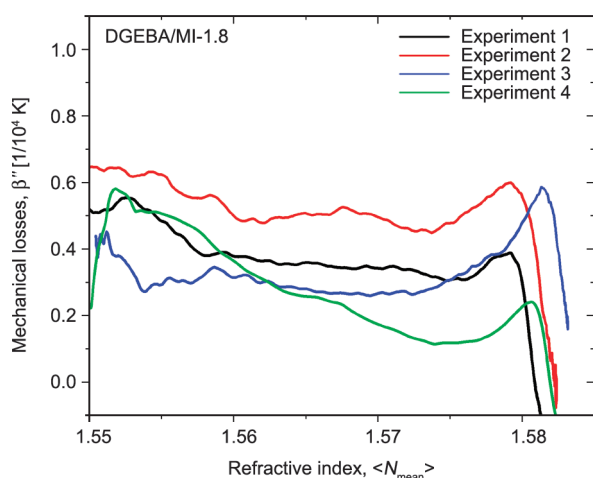


Figure 12. Collection of four individual TMOR measurements of DGEBA/MI-1.8. Shown are the mechanical loss curves as a function of the refractive index development in the course of polymerization. The datasets were obtained based on the same material batch, measured with four different TMOR refractometers.

This result clearly demonstrates that the same superimposed process ($T_{\text{iso}} = 80^\circ\text{C}$), applied to samples that have been prepared under the most identical conditions possible, leads to different glassy states due to the formation of different morphologies. However, again, it should be stressed that the dynamical glass transition, measured with a probe frequency at 17 mHz, represents still a viscoelastic and

not a solid state. In agreement with this statement, polymerization might still be possible although the volume change reflects almost solid-state properties. All over, the glass transition largely depends on the molecular bond formation path (including linear polymerization versus cross-linking) and thus underlies a certain statistical uncertainty, which needs to be kept in mind when dealing with non-equilibrium type of processes such as polymerization.

4. Conclusions

Based on a combination of TMOR and IR spectroscopy, it has been shown that the refractive index can substitute the spectroscopically measured degree of cure, over a wide range, from the initially liquid and reactive state up to the glass transition. Even more, the simultaneously assessed thermal volume expansion coefficient, as a tool to access the glass transition, can accordingly be described as a function of the chemical turnover (the refractive index), using the same experiment, even under isothermal conditions. Based on the homopolymerization of the epoxy resin, *i.e.* the exclusive loss of oxirane ring structures during polymerization, it is shown that the depletion of reactive groups measured via IR is indeed a measure to the total degree of cure, since other network-forming reactions are excluded. This means, due to the homopolymerization reaction, the changes of the

refractive index, as a measure to the electronic dipole density and the average magnitude of the electronic dipole moments, can be exclusively related to the loss of a single molecular group: the oxirane rings. Hence, this is the origin of the striking linearity between the spectroscopically measured degree of cure and the refractive index. In cases, when different reactive moieties might be involved in the polymerization process, the spectroscopically measured degree of cure is less meaningful and the linear relationship to the refractive index deviates. This argument even strengthens the usage of the refractive index as a measure to the degree of cure for all types of polymerization processes, because changes of the refractive index involve all possible changes of the underlying morphology, independent of the chemical origin.

This holds true, at least up to the glass transition, when the molecular movement is largely hindered but intra-network reactions can still occur, *e.g.* due to unreacted moieties. Such chemical reactions rather increase internal mechanical stresses than cause another change of the volume.

Within that regard, the quasi-static glass transition appears as a bending or levelling of the refractive index over u in the $N_{\text{mean}} = N_{\text{mean}}(u)$ -plot and causes the saturation of the volume shrinkage at high chemical turnovers. Nevertheless, a unique correlation between the 1-MI concentration and the polymerization-induced appearance of T_g^{stat} on the $\langle u \rangle$ -axis is not observed. However, in contrast to N_{mean} , the derived volume shrinkage seems to be more sensitive to the variations of the initiator concentration and ultimately increases from 4.8 to 5.3% with increasing initiator concentration.

Furthermore, it is found that the variation of the 1-MI concentration (up to 3.2 wt%) as an initiator to the homopolymerization reaction has neither an effect on the totally achievable degree of cure of such systems nor on the polymerization-induced dynamic glass transition, as shown by low frequency measurements ($f = 17$ mHz) of the dynamic thermal volume expansion coefficient $\beta'(u)$, for all 1-MI concentrations. This is because the glass transition itself underlies a certain statistical uncertainty, due to the morphological variation during polymerization. Here, it should be stressed that the quasi-static glass transition, as measured by Abbe refractometry, is monitored by volume changes at the transition into the solid state, whereas the chemical induced dynamic

glass transition is monitored by entropy production (β''). The quasi-static and the dynamic monitoring of the chemical induced glass transition therefore yield different perspectives on the glass transition.

Finally, there is no indication for any instantaneous structural change for the three 1-MI concentrations below the polymerization-induced dynamic glass transition. Hence, the percolation transition does not couple to the thermal volume expansion in a measurable way but remains hidden in the dynamic susceptibility of thermal volume expansion.

Acknowledgements

The authors gratefully acknowledge the discussions with Martine Philipp. Furthermore, we acknowledge the cooperation with Anton Paar OptoTec GmbH, Seelze, Germany.

References

- [1] Petrie E. M.: Epoxy adhesive formulations. McGraw-Hill, New York (2006).
- [2] Boyle M. A., Martin C. J., Neuner J. D.: Epoxy resins. in 'ASM handbook composites' (eds.: Miracle D. B., Donaldson S. L.) ASM International, Novelt, Vol. 21, 78–89 (2001).
- [3] Breuer U. P.: Commercial aircraft composite technology. Springer, Cham (2016).
- [4] Pantelakis S., Tserpes K.: Revolutionizing aircraft materials and processes. Springer, Berlin (2020).
- [5] Debenedetti P. G.: Metastable liquids: Concepts and principles. Princeton University Press, Princeton (1996).
- [6] Strobl G. R.: The physics of polymers. Springer, Berlin (2010).
- [7] Fernández-Francos X., Kazarian S. G., Ramis X., Serra À.: Simultaneous monitoring of curing shrinkage and degree of cure of thermosets by attenuated total reflection fourier transform infrared (ATR FT-IR) spectroscopy. *Applied Spectroscopy*, **67**, 1427–1436 (2013). <https://doi.org/10.1366/13-07169>
- [8] Müller U., Philipp M., Gervais P.-C., Possart W., Wehlack C., Kieffer J., Sanctuary R., Krüger J.-K.: Combination of high-performance refractometry and infrared spectroscopy as a probe for chemically induced gelation and vitrification of epoxies. *New Journal of Physics*, **12**, 083036 (2010). <https://doi.org/10.1088/1367-2630/12/8/083036>
- [9] Szymoniak P., Qu X., Abbasi M., Pauw B. R., Henning S., Li Z., Wang D.-Y., Schick C., Saalwächter K., Schönhals A.: Spatial inhomogeneity, interfaces and complex vitrification kinetics in a network forming nanocomposite. *Soft Matter*, **17**, 2775–2790 (2021). <https://doi.org/10.1039/D0SM01992E>
- [10] Sarge S. M., Höhne G., Hemminger W.: Calorimetry: Fundamentals, instrumentation and applications. Wiley-VCH, Weinheim (2014).

- [11] Skordos A. A., Partridge I. K.: Determination of the degree of cure under dynamic and isothermal curing conditions with electrical impedance spectroscopy. *Journal of Polymer Science Part B: Polymer Physics*, **42**, 146–154 (2004).
<https://doi.org/10.1002/polb.10676>
- [12] O'Brien D. J., Mather P. T., White S. R.: Viscoelastic properties of an epoxy resin during cure. *Journal of Composite Materials*, **35**, 883–904 (2001).
<https://doi.org/10.1177/a037323>
- [13] Klingler A., Gilberg M., Krüger J.-K., Wetzel B.: On volume changes during homopolymerization of polymer networks accessed *via* 'Temperature modulated optical refractometry'. *Thermochimica Acta*, **711**, 179185 (2022).
<https://doi.org/10.1016/j.tca.2022.179185>
- [14] Philipp M., Zimmer B., Ostermeyer M., Krüger J.-K.: Polymerization-induced shrinkage and dynamic thermal expansion behavior during network formation of polyurethanes. *Thermochimica Acta*, **677**, 144–150 (2019).
<https://doi.org/10.1016/j.tca.2019.01.012>
- [15] Holst M., Schänzlin K., Wenzel M., Xu J., Lellinger D., Alig I.: Time-resolved method for the measurement of volume changes during polymerization. *Journal of Polymer Science Part B: Polymer Physics*, **43**, 2314–2325 (2005).
<https://doi.org/10.1002/polb.20519>
- [16] Baur H.: *Thermophysics of polymers I*. Springer, Berlin (1999).
- [17] Haug A.: *Theoretische Festkörperphysik*. Franz Deuticke Verlag, Wien (1964).
- [18] Müller U., Philipp M., Thomassey M., Sanctuary R., Krüger J.-K.: Temperature modulated optical refractometry: A quasi-isothermal method to determine the dynamic volume expansion coefficient. *Thermochimica Acta*, **555**, 17–22 (2013).
<https://doi.org/10.1016/j.tca.2012.12.011>
- [19] Philipp M., Zimmer B., Ostermeyer M., Krüger J.-K.: Simultaneous access to the low-frequency dynamics and ultraslow kinetics of the thermal expansion behavior of polyurethanes. *Thermochimica Acta*, **686**, 178410 (2020).
<https://doi.org/10.1016/j.tca.2019.178410>
- [20] Philipp M., Nies C., Ostermeyer M., Possart W., Krüger J.-K.: Thermal glass transition beyond kinetics of a non-crystallizable glass-former. *Soft Matter*, **14**, 3601–3611 (2018).
<https://doi.org/10.1039/C7SM02359F>
- [21] dos Santos D. J., Gouveia J. R., Philipp M., Augusto A. C., Ito N. M., Krüger J.-K.: Temperature modulated optical refractometry: A novel and practical approach on curing and thermal transitions characterizations of epoxy resins. *Polymer Testing*, **77**, 105915 (2019).
<https://doi.org/10.1016/j.polymertesting.2019.105915>
- [22] Heise M. S., Martin G. C.: Curing mechanism and thermal properties of epoxy-imidazole systems. *Macromolecules*, **22**, 99–104 (1989).
<https://doi.org/10.1021/ma00191a020>
- [23] Fernández-Francos X.: Theoretical modeling of the effect of proton donors and regeneration reactions in the network build-up of epoxy thermosets using tertiary amines as initiators. *European Polymer Journal*, **55**, 35–47 (2014).
<https://doi.org/10.1016/j.eurpolymj.2014.03.022>
- [24] Ricciardi F., Romanchick W. A., Joullié M. M.: Mechanism of imidazole catalysis in the curing of epoxy resins. *Journal of Polymer Science: Polymer Chemistry Edition*, **21**, 1475–1490 (1983).
<https://doi.org/10.1002/pol.1983.170210520>
- [25] Ooi S. K., Cook W. D., Simon G. P., Such C. H.: DSC studies of the curing mechanisms and kinetics of DGEBA using imidazole curing agents. *Polymer*, **41**, 3639–3649 (2000).
[https://doi.org/10.1016/S0032-3861\(99\)00600-X](https://doi.org/10.1016/S0032-3861(99)00600-X)
- [26] Rozenberg B. A.: Kinetics, thermodynamics and mechanism of reactions of epoxy oligomers with amines. in 'Epoxy resins and composites II. Advances in polymer science' (ed.: Dušek K.) Springer, Berlin, Vol. **75**, 113–165 (1986).
- [27] Fernández-Francos X., Cook W. D., Serra À., Ramis X., Liang G. G., Salla J. M.: Crosslinking of mixtures of DGEBA with 1,6-dioxaspiro[4,4]nonan-2,7-dione initiated by tertiary amines. Part IV. Effect of hydroxyl groups on initiation and curing kinetics. *Polymer*, **51**, 26–34 (2010).
<https://doi.org/10.1016/j.polymer.2009.11.013>
- [28] Possart W., Krüger J.-K., Wehlack C., Müller U., Petersen C., Bactavatchalou R., Meiser A.: Formation and structure of epoxy network interphases at the contact to native metal surfaces. *Comptes Rendus Chimie*, **9**, 60–79 (2006).
<https://doi.org/10.1016/j.crci.2005.04.009>
- [29] Wehlack C., Possart W., Krüger J.-K., Müller U.: Epoxy and polyurethane networks in thin films on metals – Formation, structure, properties. *Soft Materials*, **5**, 87–134 (2007).
<https://doi.org/10.1080/15394450701554536>
- [30] Müller U., Krüger J.-K.: Temperature modulated refractive index measurement. EP 2609417, Germany (2013).
- [31] Heise M. S., Martin G. C.: Analysis of the cure kinetics of epoxy/imidazole resin systems. *Journal of Applied Polymer Science*, **39**, 721–738 (1990).
<https://doi.org/10.1002/app.1990.070390321>
- [32] Lorentz H. A.: Ueber die Beziehung zwischen der Fortpflanzungsgeschwindigkeit des Lichtes und der Körperdichte. *Annalen der Physik und Chemie*, **245**, 641–665 (1880).
<https://doi.org/10.1002/andp.18802450406>
- [33] Lorenz L.: Ueber die Refraktionsconstante. *Annalen der Physik und Chemie*, **247**, 70–103 (1880).
<https://doi.org/10.1002/andp.18802470905>

- [34] Böttcher C. J. F.: Theory of electric polarisation. Elsevier, Amsterdam (1952).
- [35] Wenzel M.: Spannungsbildung und Relaxationsverhalten bei der Aushärtung von Epoxidharzen. PhD thesis, Technische Universität Darmstadt (2005).
- [36] Montarnal D., Capelot M., Tournilhac F., Leibler L.: Silica-like malleable materials from permanent organic networks. *Science*, **334**, 965–968 (2011).
<https://doi.org/10.1126/science.1212648>
- [37] Kovacs A. J., Aklonis J. J., Hutchinson J. M., Ramos A. R.: Isobaric volume and enthalpy recovery of glasses. II. A transparent multiparameter theory. *Journal of Polymer Science: Polymer Physics Edition*, **17**, 1097–1162 (1979).
<https://doi.org/10.1002/pol.1979.180170701>
- [38] Debenedetti P. G., Stillinger F. H.: Supercooled liquids and the glass transition. *Nature*, **410**, 259–267 (2001).
<https://doi.org/10.1038/35065704>
- [39] Holst M.: Reaktionsschwindung von Epoxidharz-Systemen. PhD thesis, Technische Universität Darmstadt (2001).